

# Solid–liquid transition of skyrmions in a two-dimensional chiral magnet

Yoshihiko Nishikawa,<sup>1,\*</sup> Koji Hukushima,<sup>1,2,†</sup> and Werner Krauth<sup>3,4,‡</sup>

<sup>1</sup>*Department of Basic Science, Graduate School of Arts and Sciences,  
The University of Tokyo, 3-8-1 Komaba, Meguro, Tokyo 153-8902, Japan*

<sup>2</sup>*Center for Materials Research by Information Integration,  
National Institute for Materials Science, 1-2-1, Sengen, Tsukuba, Ibaraki, 305-0047, Japan*

<sup>3</sup>*Laboratoire de Physique Statistique, Département de physique de l'ENS,  
Ecole Normale Supérieure, PSL Research University,  
Université Paris Diderot, Sorbonne Paris Cité, Sorbonne Universités,  
UPMC Univ. Paris 06, CNRS, 75005 Paris, France*

<sup>4</sup>*Department of Physics, Graduate School of Science,  
The University of Tokyo, 7-3-1 Hongo, Bunkyo, Tokyo 113-0033, Japan*

(Dated: October 31, 2017)

We study the melting of skyrmions in a two-dimensional Heisenberg chiral magnet with bi-axial Dzyaloshinskii–Moriya interactions. These topological excitations may form at zero temperature a triangular crystal with long-range positional order. However, we show using large-scale Monte Carlo simulations that at small finite temperature, the skyrmions rather form a typical two-dimensional solid: Positional correlations decay with distance as power laws while the orientational correlations remain finite. At higher temperature, we observe a direct transition from this two-dimensional solid to a liquid with short-range correlations. This differs from generic two-dimensional homogeneous particle systems, where a hexatic phase is realized between the solid and the liquid.

In recent years, spin textures such as magnetic skyrmions or chiral solitons were observed in chiral magnets governed by antisymmetric Dzyaloshinskii–Moriya (DM) interactions [1–3]. In magnetic systems, skyrmions were proposed theoretically as local spin vortices [4–6] that are characterized by a topological charge. These fascinating topological excitations have since been extensively studied in experiments and through theoretical models. In three-dimensional bulk compounds such as MnSi, skyrmions are confined to a small region of the phase diagram, and they only seem to be stable in a crystalline phase [7–9]. In two-dimensional thin films, on the other hand, skyrmions can be stabilized in a wide range of temperatures and magnetic fields. A triangular skyrmion crystal was observed at very low temperature in a magnetic field [9–14]. This crystal was reported stable at finite temperature [9, 11–13, 15, 16]. Two-dimensional skyrmions also exist as isolated objects, and they can form liquids [9, 12, 15], at higher temperatures than the ordered states.

In this letter, we investigate two-dimensional skyrmions in a classical Heisenberg spin model with DM interactions. We use massive Monte Carlo simulations with a dedicated parallelized algorithms implemented on GPUs [17, 18]. Our analysis relies on the analogy of the skyrmion system with interacting particle models in two dimensions. Two-dimensional particle systems, in the absence of a periodic substrate, cannot crystallize at finite temperature, that is, develop long-range positional order [19], but they can form a solid with algebraically decaying positional correlation functions and long-range orientational order [20]. The global orientational order  $\Psi_6$  is defined as the average over all particles of the local orientational order  $\psi_j = \langle \exp(6i\theta_{jk}) \rangle_j$  where the

bracket represents the average over neighboring particles of particle  $j$  and  $\theta_{jk}$  is the bond angle between two particles  $j$  and  $k$  measured from a fixed axis. This solid first melts into a hexatic (with algebraic orientational correlations and short-range positional correlations) and then, in a second stage, into a liquid phase [21, 22]. In the liquid, all correlation functions are short-ranged. The order of the melting transitions depends on the interaction potential. For steep power-law interactions  $U(r) = \epsilon(\sigma/r)^n$  with  $n \gtrsim 6$  including the hard-core potential ( $n \rightarrow \infty$ ), the hexatic–liquid transition is of first order whereas for weaker potentials it is continuous and can be described by the KTHNY theory [23–27]. Although skyrmions are flexible extended objects each comprising a large number of spins and, strictly speaking, are metastable excitations with a finite lifetime, they can, for the aim of our analysis, be pictured as stable point particles. Furthermore, because of its nature as a collective excitation of a large number of spins on a lattice, the coupling of a skyrmion to the periodic underlying lattice is very weak. From this viewpoint, the skyrmions in the two-dimensional chiral magnet at low temperature can be interpreted as two-dimensional particles on a fine-meshed periodic substrate. At finite temperatures, skyrmions feature quasi-long-range positional order for a floating solid that is decoupled from the underlying substrate, whereas long-range positional order can be developed only if it is locked to the substrate [24, 26]. In our large systems with  $\sim 10^6$  Heisenberg spins and  $\sim 10^4$  skyrmions, we indeed identify at zero temperature a skyrmion-crystal state with locally triangular order (minimally disturbed to accommodate the substrate potential). This state is incommensurate with the substrate at all densities.

We find that commensurate square-shaped skyrmion crystals have higher energy than triangular crystals, even in the very dilute limit near the transition field at zero temperature. They are thus not realized. At finite temperature, the triangular crystal becomes a “floating” solid with local triangular symmetry. We clearly identify the algebraic decay of positional correlations in the presence of long-range orientational correlations. The very low degree of coupling of this solid to the underlying spin system is also illustrated by the fact that for a finite system the solid may vary its orientation with respect to the lattice axes. We find at finite temperature that spin-lattice-commensurate square skyrmion structures are unstable towards a locally triangular skyrmion solid with minute inhomogeneities to accommodate the underlying lattice. As predicted by theory [24, 26], we find that the solid melts in a single step into a skyrmion liquid. The intermediate hexatic phase found in particle systems is thus absent in the chiral magnet.

Our chiral Heisenberg spin model is defined by the Hamiltonian

$$H(\{\mathbf{S}_i\}) = -J \sum_{\langle i,j \rangle} \mathbf{S}_i \cdot \mathbf{S}_j - \mathbf{D}_x \cdot \sum_i \mathbf{S}_i \times \mathbf{S}_{i+\hat{x}} - \mathbf{D}_y \cdot \sum_i \mathbf{S}_i \times \mathbf{S}_{i+\hat{y}} - \mathbf{h} \cdot \sum_i \mathbf{S}_i, \quad (1)$$

where  $\mathbf{S}_i$  is a three-component vector of fixed length  $|\mathbf{S}_i| = 1$  on a site  $i$  of the two-dimensional square lattice with periodic boundary conditions. In Eq. (1), the bracket  $\langle \cdot, \cdot \rangle$  represents all neighboring pairs. The second and third terms in the Hamiltonian constitute the DM interaction. We take  $\mathbf{h}$  parallel to the  $z$ -axis,  $\mathbf{D}_x$  parallel to the  $x$ -axis,  $\mathbf{D}_y$  parallel to the  $y$ -axis, and choose  $|\mathbf{D}_x| = |\mathbf{D}_y| = J$ . This choice stabilizes Bloch-type skyrmions at low temperature in a magnetic field [28]. This model has helical, paramagnetic (skyrmion-liquid) and skyrmion-solid phases depending on temperature and the magnetic field. We especially focus on the skyrmion solid at low temperature and the higher magnetic field (see Fig. 1).

With the parameter  $D/J = 1$ , each skyrmion is composed of  $\sim 50$  spins, and encounters large free-energy barriers with respect to local changes as they appear in experiment and in local sampling algorithms. On the one hand, this large free-energy barrier stabilizes skyrmions at low temperatures on experimental lifetimes. On the other hand, this complicates Monte Carlo calculations as at low temperature, in the solid phase, the skyrmion number  $N_s$ , although not strictly stable, changes too slowly to allow its efficient sampling by our algorithms.

To overcome this problem, our Monte Carlo simulations are performed in two stages. In the first stage, we determine the thermodynamic relevant value of skyrmions  $N_s$  (equivalent to the skyrmion density) at a low target temperature  $T$  through extensive simulated annealing runs from high temperature (where  $N_s$  changes

easily) down to  $T$ . In the second stage, we compute correlation functions using Monte Carlo simulations where, in contrast, we keep the skyrmion number rigorously fixed to the thermodynamic relevant value. To do so, we compute  $N_s$  after every Monte Carlo time step (using the topological charge [29]), and reject configurations with changed skyrmion number (see the Supplemental Item 1 for details on the Monte Carlo procedure at zero and at finite temperatures). Using a local mask, we identify the center of each skyrmion as a point particle with real-valued positions and then compute high-quality spatial correlation functions at fixed  $N_s$  (see Supplemental Item 3 for a description of our algorithm to determine real-valued skyrmion positions). For the latter analysis, it is essential that different values of  $N_s$  are not folded into the analysis of correlation functions.

Solid and crystalline skyrmion states are sensitive to the boundary conditions, that is, to the shape of the simulation box. We therefore carefully choose the linear dimensions of the spin lattice in order to minimize the distortion of solid and crystalline states (see the Supplemental Item 1 for details of our Monte Carlo procedure and of the choice of system size).

At zero temperature, a single skyrmion is stable above  $h/J \simeq 0.50$  and below  $h/J \simeq 1.10$ . However, the paramagnetic solution [30] (which, at  $T/J = 0$ , is without skyrmions) has lower energy than the single-skyrmion solution above  $h_{\text{SP}}/J = 0.69$ . Below  $h/J \simeq 0.50$ , a single skyrmion is unstable and transforms into another tube-like object with the same topological charge (see Fig. 2(a)). At  $h/J \lesssim 0.50$ , very low-density skyrmion states also become unstable, but they have higher energy than skyrmion crystal states of higher density. The

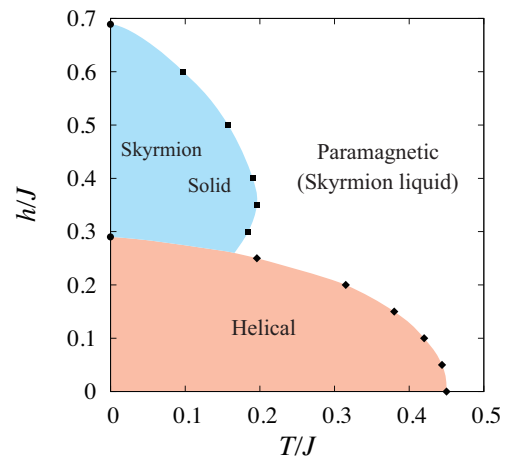


FIG. 1. Magnetic phase diagram of the two-dimensional chiral magnet. Circles correspond to zero-temperature energy minimizations. Squares are obtained by decays of correlation functions, and diamonds denote peak locations of the specific heat obtained by finite-temperature Monte Carlo simulations at each magnetic field.

latter are in fact stabilized by the mutual repulsion of skyrmions (see also [9–12, 14, 31]). Above  $h_{\text{HS}}/J \simeq 0.29$ , skyrmion crystal states thus have lower energy than the helical states of various periods (see Fig. 2(c)). We also find that square-lattice crystal configurations have higher energy than triangular lattices that minimally adjust to the substrate potential. All these crystalline and helical states are obtained by simulated annealing (SA) in magnetic field (see Supplemental Item 1 for details on the simulated annealing at zero temperature). We thus conclude at zero temperature that a triangular skyrmion crystal state (with minimal local variations) is the ground state between  $h_{\text{HS}}/J$  and  $h_{\text{SP}}/J$ , see Fig. 2(b).

At finite temperature, the correct skyrmion density at low temperature is determined by simulated annealing from high temperature (see Supplemental Item 2 for details on this simulated annealing procedure). For

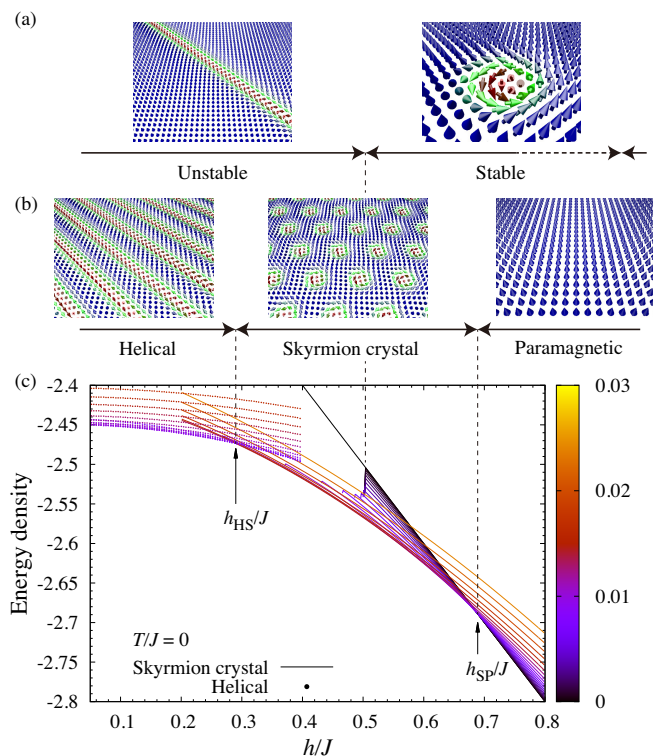


FIG. 2. (a) Phase diagram of a single skyrmion at zero temperature. For  $h/J \lesssim 0.50$ , a single skyrmion is unstable towards a tube-like object, and at high  $h/J \gtrsim 1.10$  towards the paramagnetic state. (b) Phase diagram of the system at zero temperature, with helical, triangular skyrmion crystal, and paramagnetic state ( $h_{\text{HS}}/J \simeq 0.29$  and  $h_{\text{SP}}/J \simeq 0.69$ ). (c) Energy densities of triangular skyrmion crystal states (with various densities) and helical states (with various winding numbers). The color represents the skyrmion densities for skyrmion crystal states, and square of winding densities for helical states, respectively. Square skyrmion crystals always have higher energies than the triangular skyrmion-crystal state of lowest energy.

$T/J = 0.155$  and  $h/J = 0.5$ , for example, we estimate the correct number to be  $128 \times 128$  for  $L_x = 1164$  and  $L_y = 1008$ . This value remarkably corresponds to the zero-temperature value. In order to determine spatial correlations of orientational and positional order, as described, we thus freeze the skyrmion number to the value found by simulated annealing. At low temperature, the global orientational order  $\Psi_6$  may be in different “lobes” that correspond to slight rearrangements of the skyrmion system with respect to the simulation box (see Fig. 3(a)). It is only at near-zero temperature that the number of sampled lobes in the histogram shrinks to one, as the orientational order is then locked into the value of the initial configuration. We compute the two-dimensional positional correlation function  $g(x, y)$  separately for each lobe, as each of the orientations leads to distinct distortions. (Each configuration is rotated by  $-\arg(\Psi_6)/6$  so that the resultant  $\Psi_6$  is approximately parallel to the  $x$  axis [21]). The positional correlation function  $g(x, 0) - 1$  for the lobe at  $\text{Im}\Psi_6 \simeq 0$ , at  $T/J = 0.155$  and  $h/J = 0.5$  clearly decays algebraically, with an exponent about 0.5 (Fig. 3(e)). At first sight, the positional correlation functions for other lobes appear to decay faster than algebraic at large distance. However, this is an artifact due to the slight distortion of the correlation peaks near the  $x$  axis that is caused by the mismatch of the locally triangular structure with the simulation box if  $\text{Im}\Psi_6 \neq 0$  (see the insets of Fig. 3(b)–(e)). The maximum values for all peaks, determined individually, indeed decay algebraically for all the lobes (see black open symbols in Fig. 3(b)–(d)). The correlation function of the orientational order parameter  $g_6(r)$  at this temperature converges to a constant value at a large distance that means  $g_6(r)$  has long-range correlations (Fig. 4(a)). These orientational correlations are also observed in a smaller system with  $582 \times 504$  spins and  $64 \times 64$  skyrmions, and they are consistent with an algebraic decay with exponent  $\simeq 0.5$  in the positional correlation function. Therefore we conclude that skyrmions do not form a crystal but a solid at low temperature. While the positional correlation function shows a clear algebraic decay, the exponent 0.5 is larger than the exponent  $1/3$  that is the stability limit of the solid phase predicted by the KTHNY theory. Our system has no continuous symmetry, and each position of skyrmions has small but finite coupling to the lattice sites (see Supplemental Item 4 for details on the coupling between the skyrmion positions and the substrate). This coupling can be considered as an effective periodic potential incommensurate to the skyrmion solid that stabilizes the solid phase with a larger exponent than that observed in particle systems. A larger exponent was also reported in an experimental work on a melting transition of atoms on a two-dimensional periodic substrate [32].

In the solid phase, where the positional correlations decay algebraically (see Fig. 3), orientational correlations  $g_6(r)$  are long-ranged, whereas, in the liquid, orienta-

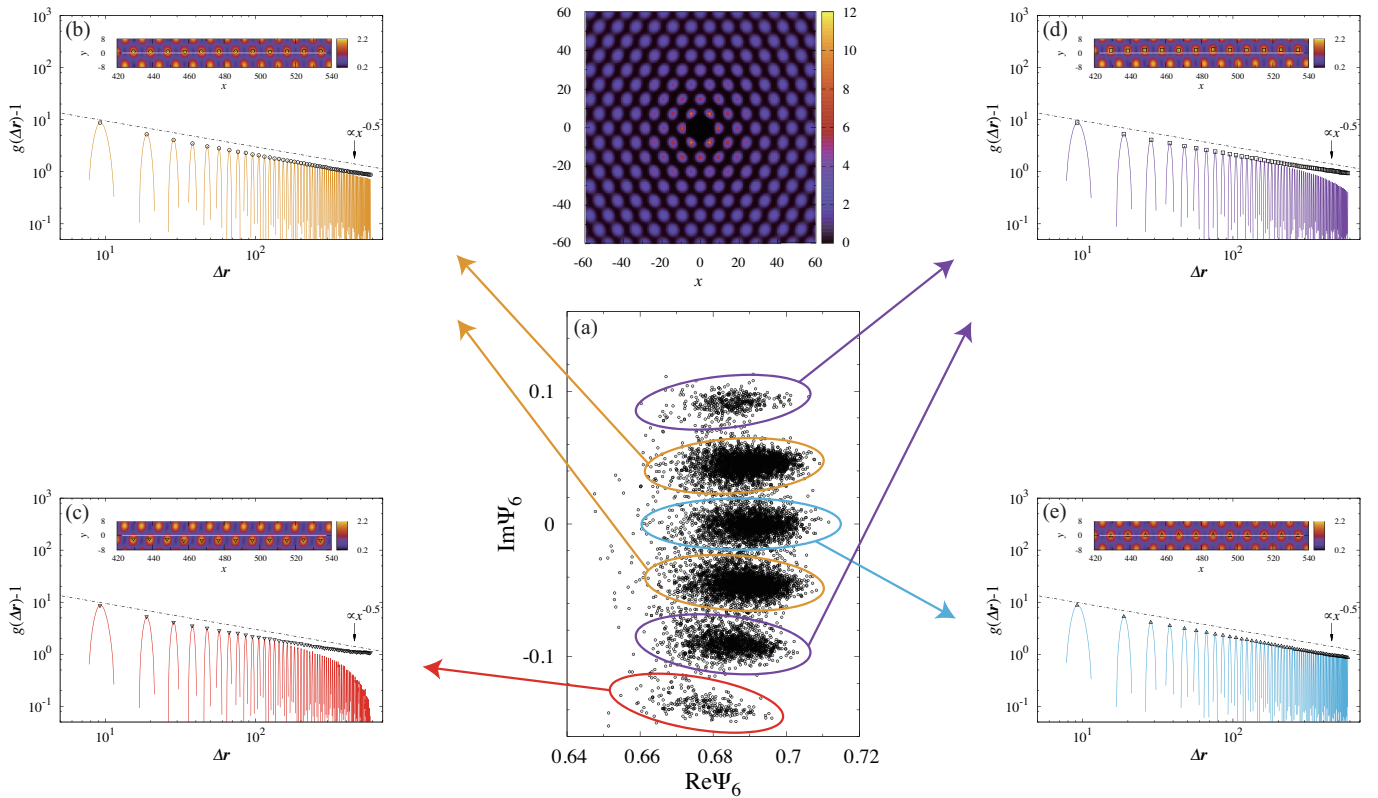


FIG. 3. (a) Scatter plot of the global bond-orientational order parameter  $\Psi_6$ , and the two-dimensional pair correlation function. (b)–(e) Positional correlation function  $g(\Delta\mathbf{r}) - 1$  for each lobe of the scatter plot. Solid lines represent  $g(x, 0) - 1$  and black open symbols (circles in (b), inverted triangles in (c), etc.) represent the maximum value of each peak in the two-dimensional correlation function  $g(x, y)$ . Insets in (b)–(e) show the two-dimensional correlation function  $g(x, y)$  near the  $x$  axis (compare with (a)). The white line is the  $x$  axis along which  $g(x, 0) - 1$  is plotted. Black open symbols again represent local maxima. The system is  $L_x = 1164$  and  $L_y = 1008$  at  $T/J = 0.155$  and  $h/J = 0.5$ .

tional correlations (as all other correlations) decay exponentially. Near the transition between the two phases, we observe, from the solid, a decrease of the asymptotic correlation  $g_6$ , and from the liquid a very rapid increase of the orientational correlation length towards a value on order of the system size  $L$  (see, for example, Fig. 4(a) at  $h/J = 0.5$ , where the transition is at  $T/J \simeq 0.16$ ). Analogous behavior is found for all other values of  $h/J$  with a solid–paramagnet transition. Unlike for the two-dimensional particle models, but in agreement with theoretical predictions [24, 26], we find no evidence of a hexatic phase. This is also consistent with the experimental work [32] that reports a direct melting transition from the solid to the liquid. Typically, the skyrmion solid melts into the paramagnet with increasing  $h/J$ , as the paramagnetic state favors magnetic order. However, in a small region of the phase diagram, the paramagnet is switched from the paramagnet into the skyrmion-solid phase on increasing the magnetic field (see Fig. 1). Accordingly, at a finite temperature, the orientational correlation functions are long-ranged at higher  $h/J$  and exponentially decaying at lower  $h/J$  (see Fig. 4(b)).

In conclusion, we have numerically studied phase transitions of skyrmions in a two-dimensional chiral Heisenberg system using massive Monte Carlo simulations at zero and at finite temperature with a dedicated algorithm that avoids the difficulty of relaxation to equilibrium due to the long skyrmion life time. We confirm that the ground state of the system is a triangular skyrmion crystal state with long-range positional order. A spin-lattice compatible skyrmion crystal is energetically unfavorable. However, the ordered skyrmion state at finite temperature is a “floating” solid, that is locally triangular, and has long-range orientational correlations yet only quasi-long-range positional correlations. The skyrmion ground state is continuously reached from the solid as the correlation length becomes ever larger. On increasing the temperature, the skyrmion solid directly melts into the liquid without an intermediate hexatic phase as it is realized in generic two-dimensional particle systems. We note that the DM interaction  $D/J = 1$  in our system is larger and the size of each skyrmion smaller than that observed in experimental compounds [9, 28]. The coupling between the location of each skyrmion and the lattice sites be-

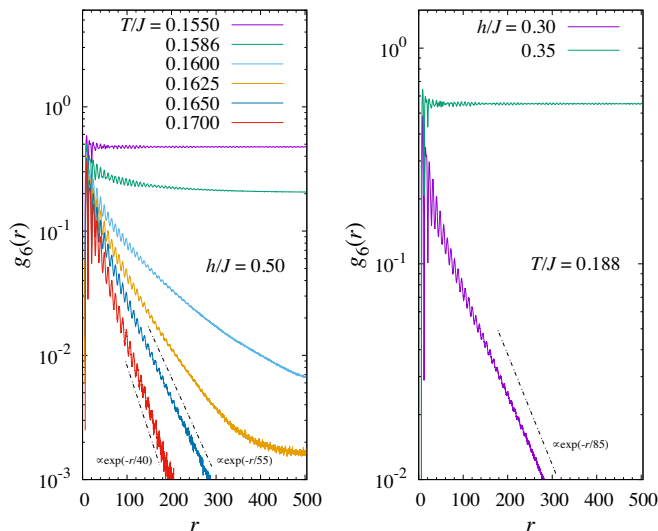


FIG. 4. Correlation function of the orientational order  $g_6(r)$  of the system with  $L_x = 1164$  and  $L_y = 1008$  at various temperatures. The magnetic field is (a)  $h/J = 0.5$ , and (b)  $h/J = 0.30$  and  $0.35$ .

comes weaker for smaller  $D/J$  and larger skyrmion, and it vanishes in the continuum model with  $D/J \rightarrow 0$  limit where the melting scenario in two-dimensional particles is expected to hold. Therefore we can expect that our results for the low-temperature solid phase with  $D/J = 1$  also hold for the case with smaller but finite  $D/J$ .

The authors thank Yusuke Masaki for many useful discussions. This work was supported by a Grant-in-Aid for JSPS Fellows (Grant No. 17J10496) and a Grant-in-Aid for Scientific Research (No. 25610102).

\* nishikawa@huku.c.u-tokyo.ac.jp

† hokusima@phys.c.u-tokyo.ac.jp

‡ werner.krauth@ens.fr

- [1] I. Dzyaloshinsky, J. Phys. Chem. Solids **4**, 241 (1958).
- [2] T. Moriya, Phys. Rev. Lett. **4**, 228 (1960).
- [3] T. Moriya, Phys. Rev. **120**, 91 (1960).
- [4] A. Bogdanov and D. A. Yablonskii, Sov. Phys. JETP **68**, 101 (1989).
- [5] A. Bogdanov and A. Hubert, J. Magn. Magn. Mater. **138**, 255 (1994).
- [6] U. K. Röbller, A. N. Bogdanov, and C. Pfleiderer, Nature **442**, 797 (2006).
- [7] K. Kadowaki, K. Okuda, and M. Date, J. Phys. Soc. Jpn. **51**, 2433 (1982).
- [8] S. Mühlbauer, B. Binz, F. Jonietz, C. Pfleiderer, A. Rosch, A. Neubauer, R. Georgii, and P. Boni, Science **323**, 915 (2009).
- [9] N. Nagaosa and Y. Tokura, Nat. Nanotechnol. **8**, 899 (2013).
- [10] S. D. Yi, S. Onoda, N. Nagaosa, and J. H. Han, Phys. Rev. B **80**, 054416 (2009).
- [11] J. H. Han, J. Zang, Z. Yang, J.-H. Park, and N. Nagaosa,

Phys. Rev. B **82**, 094429 (2010).

- [12] X. Z. Yu, N. Kanazawa, Y. Onose, K. Kimoto, W. Z. Zhang, S. Ishiwata, Y. Matsui, and Y. Tokura, Nat. Mater. **10**, 106 (2011).
- [13] S. Seki, X. Z. Yu, S. Ishiwata, and Y. Tokura, Science **336**, 198 (2012).
- [14] A. K. Nandy, N. S. Kiselev, and S. Blügel, Phys. Rev. Lett. **116**, 177202 (2016).
- [15] X. Z. Yu, Y. Onose, N. Kanazawa, J. H. Park, J. H. Han, Y. Matsui, N. Nagaosa, and Y. Tokura, Nature **465**, 901 (2010).
- [16] L. Kong and J. Zang, Phys. Rev. Lett. **111**, 067203 (2013).
- [17] M. Weigel, Comput. Phys. Commun. **182**, 1833 (2011).
- [18] M. Weigel, J. Comput. Phys. **231**, 3064 (2012).
- [19] N. D. Mermin and H. Wagner, Phys. Rev. Lett. **17**, 1133 (1966).
- [20] N. D. Mermin, Phys. Rev. **176**, 250 (1968).
- [21] E. P. Bernard and W. Krauth, Phys. Rev. Lett. **107**, 155704 (2011).
- [22] S. C. Kapfer and W. Krauth, Phys. Rev. Lett. **114**, 035702 (2015).
- [23] J. M. Kosterlitz and D. J. Thouless, J. Phys. C: Solid State Phys. **6**, 1181 (1973).
- [24] B. I. Halperin and D. R. Nelson, Phys. Rev. Lett. **41**, 121 (1978).
- [25] A. P. Young, Phys. Rev. B **19**, 1855 (1979).
- [26] D. R. Nelson and B. I. Halperin, Phys. Rev. B **19**, 2457 (1979).
- [27] J. M. Kosterlitz, Rep. Prog. Phys. **79**, 026001 (2016).
- [28] I. Kézsmárki, S. Bordács, P. Milde, E. Neuber, L. M. Eng, J. S. White, H. M. Rønnow, C. D. Dewhurst, M. Mochizuki, K. Yanai, H. Nakamura, D. Ehlers, V. Tsurkan, and A. Loidl, Nat. Mater. **14**, 1116 (2015).
- [29] B. Berg and M. Lüscher, Nuclear Physics B **190**, 412 (1981).
- [30] The paramagnetic phase at zero temperature is often incorrectly referred as the ferromagnetic phase.
- [31] J. Iwasaki, M. Mochizuki, and N. Nagaosa, Nat. Commun. **4**, 1463 (2013).
- [32] N. N. Negulyaev, V. S. Stepanyuk, L. Niebergall, P. Bruno, M. Pivetta, M. Ternes, F. Patthey, and W.-D. Schneider, Phys. Rev. Lett. **102**, 246102 (2009).

## Supplemental Item 1: Detailed parameters for the Monte Carlo code

### *Choice of lattice parameters*

For probing solid skyrmion states with locally triangular structure and their melting into a liquid, we choose a periodic rectangular spin lattice with  $L_x = k \times 97$  and  $L_y = k \times 84$  with integer  $k$ . This realizes a ratio  $L_y/L_x = 0.865979\dots$  very close to  $\sqrt{3}/2 = .866025\dots$ , and the distortion is minimal for a triangular skyrmion crystal (in “base” configuration) with  $N_{\text{sk}} = n \times n$  skyrmions with even  $n$  ( $n$  rows in the  $y$  direction of  $n$  skyrmions in the  $x$  direction). To probe helical skyrmion states with  $\pm 45^\circ$  tilting as well as crystal skyrmion states with square-lattice structure, we rather use square-shaped spin lattices with linear length  $L$ .

### *Energy minimization and simulated annealing in magnetic field at $T/J = 0$*

At zero temperature, energy minimization and simulated annealing in magnetic field are performed by the zero-temperature heat-bath algorithm (where spins are aligned with their molecular field produced by neighboring spins and by the external magnetic field  $h$ ). This produces the zero-temperature phase diagram (see Fig. 2 of the main text). We typically use  $4 \times 10^3$  sweeps to minimize the energy of the system at each magnetic field. Triangular-crystal and square-shaped skyrmion initial configurations at various densities are pieced together from individual skyrmions placed very close to the corresponding lattice sites (each individual skyrmion is prepared in a small system with  $7 \times 7$  spins at  $h/J = 0.6$ ). The helical initial configurations for Fig. 2(b) are prepared at  $h/J = 0$  from a single wave vector  $2m\pi(1, 1)/L$  with integer  $m$  and then relaxed through the zero-temperature heat-bath algorithm. Simulated annealing in  $h$  with steps of size  $|\Delta h/J| = 0.001$  then leads from  $h/J = 0.6$  to lower  $h$ , and from  $h/J = 0$  to higher  $h$  for for triangular skyrmion crystal states, and from  $h/J = 0$  to higher magnetic field for helical states (see Fig. 2 of the main text). This yields the energies for helical, triangular-crystal and square-crystal states, as well as for the paramagnetic state. System sizes are  $(L_x, L_y) = (291, 252)$  for triangular skyrmion crystals, and  $L = 256$  for helical states and for square skyrmion crystals.

### *Monte Carlo parameters at finite temperature*

In our computations of the correlation functions at finite temperature, one unit of Monte Carlo time consists of one heat-bath sweep and of  $10^4$  over-relaxation sweeps, where one sweep denotes one update per spin. We use GPUs to simulate the system with the checkerboard decomposition [17, 18]. Each block of the checkerboard consists of  $16 \times 16$  spins. As the lattice dimensions  $L_x$  and  $L_y$  are not necessarily multiples of the block size, the checkerboard is randomly shifted after every  $10^2$  over-relaxation sweeps in order to assure the ergodicity of the algorithm.

Because of the anisotropic shape of the underlying rectangular lattice, the number of skyrmions is incommensurate with the “tip” crystalline configuration with  $\text{Re}\Psi_6 < 0$ , and the lattice structure of  $g(x, y)$  would be strongly distorted, resulting in a higher energy. We thus focus on “base” configurations which minimize the distortion with the underlying spin lattice.

## Supplemental Item 2: Cooling-rate dependence of the number of skyrmions

In our production runs, the skyrmion number is kept rigorously fixed at what we believe to be the thermodynamically relevant value. To determine this dominant density of skyrmions at finite temperature, we run simulated annealing (SA) simulations from high temperature. In our SA at  $h/J = 0.5$  starting from  $T/J = 0.955$  to  $0.155$  with  $\Delta T/J = 0.01$ , the number of Monte Carlo steps at each temperature  $M$  is controlled, where one Monte Carlo time step consists of one heat-bath sweep followed by ten over-relaxation sweeps. The resultant skyrmion number  $N_s$  decreases with decreasing the cooling rate  $\theta = (\Delta T/J)/M$  (see Fig. S1). The equilibrium density of skyrmions is obtained in the limit of vanishing cooling rate.  $N_s$  approaches  $128 \times 128$  in this limit for the system with  $L_x = 1164$  and  $L_y = 1008$ . For smaller systems with  $(L_x, L_y) = (582, 504)$  and  $(291, 252)$ , the same limiting density is obtained.

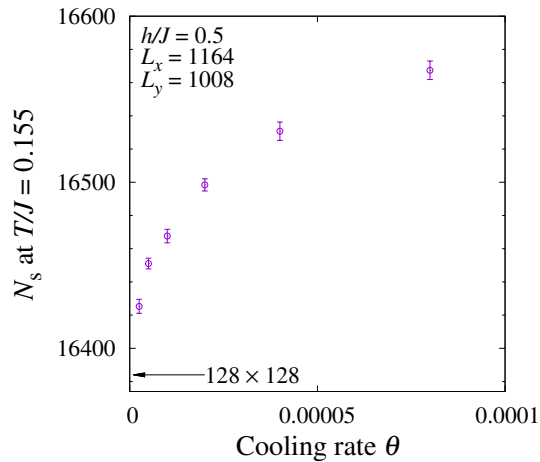


FIG. S1. Cooling-rate dependence of the number of skyrmions in configurations at  $T/J = 0.155$  obtained by simulated annealing simulations from a high temperature. The magnetic field  $h/J = 0.5$ . The leftmost point  $\theta = 0$  corresponds to the equilibrium limit.

### Supplemental Item 3: Determining the position of a single skyrmion

Although each skyrmion is composed of Heisenberg spins on a discrete square lattice, we may assign it a real-valued position  $((x, y))$ . This allows us to effectively map the Heisenberg-spin model to a model of interacting particles and to compute positional and the bond-orientational order, in analogy to what is done for two-dimensional particle systems. At zero temperature, an isolated skyrmion has a symmetric structure around its core, and spins near a core of a skyrmion are antiparallel to the magnetic field (they thus point into the  $-z$  direction). We thus consider a connected cluster of spins with  $S_i^{(z)} < 0$  as a skyrmion, and define the position of the skyrmion  $\mathbf{R}_{\text{sk}}$  in the two-dimensional plane as

$$R_{\text{sk}}^{(\alpha)} = \frac{1}{A_{\text{sk}}} \sum_{i \in \text{skyrmion}} \left( r_i^{(\alpha)} + S_i^{(\alpha)} \right), \quad (\alpha = x, y) \quad (\text{S1})$$

where  $A_{\text{sk}}$  is the number of spins composing the skyrmion. At finite temperature, the thermal fluctuations of the Heisenberg spins induce fluctuations in the determination of the skyrmion position.

### Supplemental Item 4: Coupling between skyrmion positions and the spin lattice

The skyrmion locator of Eq. (S1) allows us to compute the coupling potential between skyrmion locations and spin lattice sites. We simulate one single skyrmion in the system with  $16 \times 16$  spins at  $T/J = 0.1$  to obtain a histogram of the skyrmion locations

$$P(\Delta\mathbf{r}) = \left\langle \delta \left( \Delta\mathbf{r} - \min_k (\mathbf{R}_{\text{sk}} - \boldsymbol{\ell}_k) \right) \right\rangle,$$

where the bracket  $\langle \dots \rangle$  represents average over configurations with only one skyrmion, and  $\boldsymbol{\ell}_k$  represents the location of  $k$ -th lattice site. Then, the coupling potential is estimated as  $V_{\text{coup}}(\Delta\mathbf{r}) = -\log(P(\Delta\mathbf{r}))/\beta$ . Fig. S2 shows  $V_{\text{coup}}(\Delta\mathbf{r})$  at various magnetic fields. The coupling potential is clearly nonzero. Furthermore, the potential minimum depends on the magnetic field (see Fig. S2). We checked that the coupling potential is independent of system size.

### Supplemental Item 5: Phase diagram of the system

Transition temperatures between the paramagnetic and the helical phases in the phase diagram Fig. 1 are estimated as the peak locations of the specific heat. We perform regular Monte Carlo simulations using the heat-bath, the over-relaxation, and the exchange Monte Carlo (parallel tempering) algorithms. System sizes range from  $L = 32$  (the total

number of spins is  $N = 1024$  to  $L = 256$  ( $N = 65536$ ). The number of Monte Carlo sweeps is typically  $10^5$ . We checked that the peak location of the specific heat varies very little with the system size, up to  $L = 256$ .

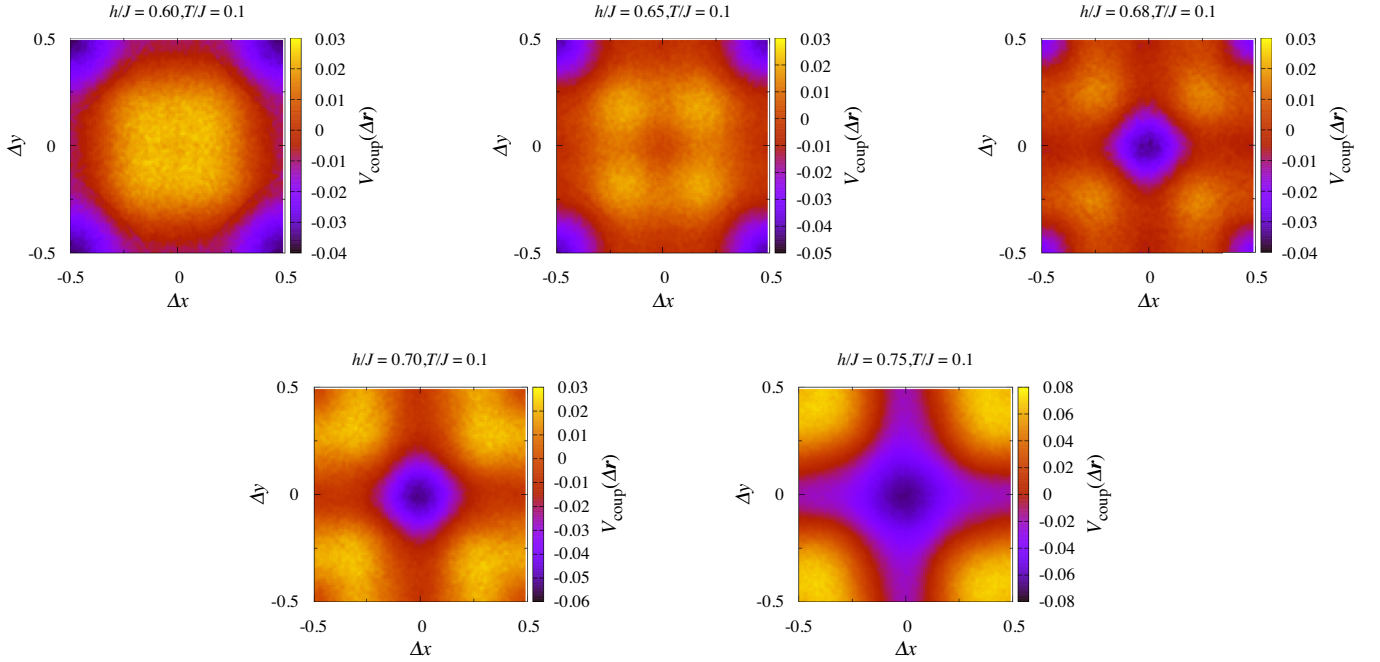


FIG. S2. Effective coupling potential  $V_{\text{coup}}(\Delta\mathbf{r})$  characterizing the coupling between skyrmion positions and lattice sites. For  $h/J \gtrsim 0.68$ , the potential minimum coincides with the lattice sites ( $\Delta x = \Delta y = 0$ ), but at smaller magnetic field, the minimum lies between the lattice spins, at  $\Delta x = \Delta y = 0.5$ .